Mapping the peptide and protein immune response in the larvae of the fleshfly *Sarcophaga bullata*

ALICE CIENCIALOVÁ,[a] TEREZA NEUBAUEROVÁ,[b] MILOSLAV ŠANDA,[a] RADEK ŠINDELKA,[c] JOSEF CVAČKA,[a] ZDENĚK VOBURKA,[a] MILOŠ BUDĚŠÍNSKÝ,[a] VÁCLAV KAŠIČKA,[a] PETRA SÁZELOVÁ,[a] VERONIKA ŠOLÍNOVÁ,[a] MARTINA MACKOVÁ,[b] BOHUMÍR KOUTEK[a] and JIŘÍ JIRÁČEK[a]*

[a] Institute of Organic Chemistry and Biochemistry, Academy of Sciences of the Czech Republic, Flemingovo nám. 2, 166 10 Praha 6, Czech Republic
[b] Institute of Chemical Technology Prague, Faculty of Food and Biochemical Technology, Technická 5, 166 28 Praha 6, Czech Republic
[c] Institute of Molecular Genetics, Academy of Sciences of the Czech Republic, Vídeňská 1083, 142 20 Praha 4, Czech Republic

Abstract: We chose the larvae of fleshfly *Sarcophaga bullata* to map the peptide and protein immune response. The hemolymph of the third-instar larvae of *S. bullata* was used for isolation. The larvae were injected with bacterial suspension to induce an antimicrobial response. The hemolymph was separated into crude fractions, which were subdivided by RP-HPLC, gel electrophoresis, and free-flow electrophoresis. In several fractions, we determined significant antimicrobial activities against the pathogenic bacteria *Escherichia coli*, *Staphylococcus aureus*, or *Pseudomonas aeruginosa*. Among antimicrobially active compounds we identified dipeptide β-alanyl-L-tyrosine, protein transferrin, and two variants of peptide sapecin. We also partially characterized two novel antimicrobially active polypeptides; odorant-binding protein 99b, and a peptide which remains unidentified. Copyright © 2007 European Peptide Society and John Wiley & Sons, Ltd.

INTRODUCTION

Disease-causing microbes resistant to drug therapy are an increasing public health problem. Tuberculosis, gonorrhea, and childhood ear infections are just a few examples of diseases that have become difficult to treat with antibiotics. The World Health Organization (WHO, Geneva) estimates that 1 500 people die each hour from an infectious disease, half of these being children under 5 years of age. Today, nosocomial infections affect over 2 million patients annually in the USA, at a cost in excess of $4.5 billion [1]. The growing problem of microbial resistance to conventional antibiotics and the need for new antibiotics, especially with new mechanisms of action, has stimulated interest in the development of antimicrobial peptides as human therapeutics [2,3].

Peptides and polypeptides with antimicrobial activity can be classified on the basis of their biochemical and structural features, the largest group of which concerns the so-called cationic peptides, which are widely distributed in plants, animals and bacteria [4]. Currently, more than 1000 naturally occurring antimicrobial peptides are known [5–7] and are typically positively-charged and composed of 10–40 amino acids, approximately 50% of which consists of hydrophobic residues. These properties confer their amphipathic character [6]. Cationic peptides are grouped into three families on the basis of their secondary structure: (i) linear peptides with an α-helical conformation (cecropins) [8], (ii) cyclic and open-ended cyclic peptides with pairs of cysteine residues (defensins) [9–11], and (iii) peptides with over-representation of amino acid proline (pyrrhocoricin) [12–14] or glycine (attacin) [1].

Three other classes of antimicrobial peptides have been recently isolated from different invertebrate and vertebrate species: anionic peptides, aromatic dipeptides, and peptides derived from oxygen-binding proteins [4]. The anionic peptides are generally isolated from mammalian epithelia (e.g. enkelytin) [15], peptide B [16], or aspartic acid-rich peptides [17]. The aromatic dipeptides consist of low molecular weight compounds such as *N*-β-alanyl-5-*S*-glutathionyl-3,4-dihydroxyphenylalanine identified in fleshfly *Sarcophaga peregrina* [18] and *p*-hydroxycinnamaldehyde that was isolated from the saw fly *Acantholyda parki* [19]. The dipeptide β-alanyl-tyrosine with modest antimicrobial activity has been constitutively found in the fleshfly *Neobellieria bullata* [20]. Hemocyanin derivatives, the peptides derived from oxygen-binding proteins, were recently isolated from the hemolymph of arthropods. The proteolyzed form of vertebrate hemoglobin with antimicrobial activity was detected in the tick *Boophilus microplus* [21].

There are different modes of action of antimicrobial peptides. The majority of cationic antimicrobial

* Correspondence to: Jiří Jiráček, Institute of Organic Chemistry and Biochemistry, Academy of Sciences of the Czech Republic, Flemingovo nám. 2, 166 10 Praha 6, Czech Republic; e-mail: jiracek@uochb.cas.cz

peptides is known to selectively target the negatively charged lipid bilayer of bacterial cells [22,23] and do not interact with the outer membrane of mammalian cells, which is zwitterionic. Nevertheless, the membrane permeabilization alone appears insufficient to cause cell death [24,25]. Other events such as membrane dysfunction, inhibition of synthesis of extracellular biopolymers [26,27], or inhibition of intracellular processes are necessary for an effective antimicrobial activity. Alternatively, antimicrobial peptides can serve to control proteinases involved in inflammatory processes. Examples include the inhibition of furin by histatin 3 [28] or inhibition of cathepsin L by probactenecin 5 from bovine neutrophils [29].

Microbiological and biophysical studies typically examine biological activities of individual antimicrobial peptides to minimize experimental variability. However, as it inevitably occurs in nature, antimicrobial peptides may interact simultaneously with microbial pathogens in a variety of settings, including complex mixtures of peptides within phagolysosomes or in the extracellular milieu. In 2001, Yan and Hancock demonstrated that various antimicrobial peptides function synergistically with lysozyme *in vitro* [30].

Insects are the largest and the most diverse group of animals living on earth [31]. Approximately 800 000 insect species, about 80% of all the animal species known to date, have been identified and classified [32]. Insects are usually exposed to a wide range of microbes throughout their life cycle and some insect species feed on animal tissues or excrements infected with microorganisms and parasites. The amazing diversity and evolutionary success of insects argue for an effective system of defense against microbes [33]. Insects have evolved powerful defense systems based on an innate immunity that relies mainly on the synthesis of proteins, peptides, as well as small organic molecules. Thus, insects may represent a unique and vast source of novel potential therapeutics [31]. The diversity of amino acid sequences is so large that the same peptides are rarely recovered from two different species of an animal, even those that are closely related. The diversity may reflect the species' adaptation to the unique microbial environment [2,32].

In insects, rapid humoral response reactions are triggered by wound or microbial infection. The most immediate response occurs within minutes and consists of the activation of prophenoloxidase activating enzyme (PPAE) that converts prophenoloxidase to phenoloxidase [33]. Phenoloxidase is an enzyme involved in melanin biosynthesis and is also important in cuticular sclerotization, wound healing, and in the encapsulation of foreign material [34,35]. The humoral response includes the production of lectins and rapid *de novo* synthesis of antimicrobial peptides by the fat body, the functional homologue of the mammalian liver, and by the hemocytes [36,37]. Studies on *Drosophila* mutants revealed that Toll and Imd pathways control the synthesis of specific gene-encoded antimicrobial peptides. The Toll pathway is activated by and against Gram-positive bacteria and fungi. The Imd pathway governs defense reactions against Gram-negative bacteria [38–41].

We have chosen larvae of fleshfly *Sarcophaga bullata* to map the immune response and for the isolation and characterization of new antimicrobial compounds. The larval development in the fleshfly proceeds in three larval instars. The female deposits live larvae that moult into the second instar in about 18–24 h and into the third instar 40–48 h after larviposition. Most of the feeding is done during the third instar, which lasts approximately 3–4 days [42]. For our experiments we used larvae hemolymph, the body fluid where antimicrobial compounds are secreted and accumulated [43]. Hemolymph was obtained from wandering third-instar larvae, i.e. larvae that left the food and sought for dry places to pupariate. In this study we present two different isolation protocols, which resulted in the identification of several previously known as well as two novel antimicrobial proteins.

MATERIALS AND METHODS

Fleshfly Larvae

S. bullata fleshflies were grown under laboratory conditions, as previously described [44]. Briefly, 200–300 larvae specimens of *S. bullata* were grown on beef liver in small open disposable packets made from aluminium foil at $25 \pm 1\,°C$.

Induction of Larvae by Bacterial Suspension and Isolation of Larval Hemolymph

Before induction, larvae had been immobilized by chilling on ice. Bacterial suspensions of *Escherichia coli* were injected into the abdomen of the larvae during their third-instar wandering period using either a calibrated glass capillary with a finely drawn tip or entomological pin. Bacteria used for induction were cultivated in a Luria-Bertani broth at $37\,°C$ for 12 h to the mid-exponential phase of growth and were at a final concentration of 10^9 cfu/ml. After cultivation the cells were centrifuged at 3 000 g for 10 min and washed twice with 0.1 M phosphate buffer pH 7.0. The cells were diluted in physiological saline until the final absorbance was 1.5–1.8 at 550 nm. We used intact larvae as a control to distinguish the immune response.

Isolation of Larval Hemolymph

After 22 h of induction, the hemolymph from induced and control larvae were collected on ice. The cells and debris were removed by an initial centrifugation for 10 min at 1000 *g* and $4\,°C$. The resulting supernatant was precipitated either by four volumes of acidic methanol (90% methanol, 9% distilled water, and 1% acetic acid, v/v/v) or by ammonium sulfate (saturation to 70%). The precipitates were centrifuged for 30 min at 13 000 *g* at $4\,°C$.

Chromabond C-18 Cartridges - Solid-Phase Extraction

Supernatants resulting from either acidic methanol or ammonium sulfate precipitation were divided into hydrophilic and hydrophobic fractions using Chromabond C-18 cartridges (Macherey-Nagel, Germany). Methanol was removed from the supernatant by evaporation and the residue was dissolved in 0.1% v/v aqueous TFA. Chromabond C-18 cartridges were activated by 80% v/v aqueous acetonitrile, rinsed with water and the samples were loaded repeatedly. Hydrophilic fractions were obtained using 0.1% TFA elution. Hydrophobic fractions were eluted from cartridges by 80% aqueous acetonitrile. All fractions were evaporated using a Speed-vac.

Reversed Phase-High Performance Liquid Chromatography

Hydrophilic and hydrophobic fractions were further analyzed and subdivided using RP-HPLC with apparatus Waters 600 and C-18 columns Vydac 218TP54 (250×4 mm, 5 µm) or Vydac 218TP54 (250×10 mm, 5 µm). Elution was achieved by a gradient with rising concentration of acetonitrile in water in the presence of 0.1% TFA. Chromatograms were analyzed using Empower software (Waters, USA) or DataApex Clarity Lite software, (DataApex, Czech Republic).

Electrospray Ionization Mass Spectrometry (ESI-MS) for Identification of Low Molecular Weight Compounds

Mass spectra of the isolated fractions and synthetic analogs were recorded using a quadrupole orthogonal acceleration time-of-flight tandem mass spectrometer Q-TOF Micro (Waters). Samples dissolved in acetonitrile/0.2% formic acid in water (1 : 1, v/v) were injected into the mobile phase of the same composition at a flow rate of 20 µl/ min. The electrospray ion source was operated in positive ion mode with capillary voltage and cone voltage at 3500 and 20 V, respectively. Nitrogen was used as the cone gas (50 l/h) and desolvation gas (150 l/h). The source and desolvation temperature was 80 and 150 °C, respectively. In the MS mode, the collision energy was set at 10 V; the value was increased, typically to 15–25 V, for MS/MS experiments.

MALDI Ionization Mass Spectrometry for Determination of Relative Molecular Weight of Proteins and Peptides

Mass spectra of individual fractions were measured by a MALDI-TOF mass spectrometer REFLEX IV (Brüker-Daltonic) equipped with N_2 laser (337 nm). Mass spectra were acquired in the linear mode with an acceleration voltage of 20 kV. Sinapinic acid was used as the matrix.

Identification of Peptides and Proteins from Proteolytic Digests by Mass Spectrometry Techniques

Selected protein or peptide bands from 1D-SDS PAGE were cut, destained using 50% acetonitrile in 25 mM ammonium bicarbonate buffer pH 7.8 or in 50 mM 4-ethylmorpholine acetate buffer pH 8.1 with 40 mM DTT, dehydrated with 200 µl of acetonitrile for 5 min at 30 °C using a thermo shaker (Eppendorf) at 30 °C and then vacuum dried in a Speed-vac (Labconco). Gel pieces were rehydrated and proteins/peptides were digested with the Cleavage buffer 1 or 2 using the thermo shaker for 8 h at 37 °C. Cleavage buffer 1 contained 30 ng/µl of enzyme in 50 mM 4-ethylmorpholine acetate pH 8.1, 4% acetonitrile, and 0.01% β-mercaptoethanol. Cleavage buffer 2 contained 30 ng/µl of enzyme in 25 mM ammonium bicarbonate pH 7.8, 4% acetonitrile, and 0.01% β-mercaptoethanol. Trypsin (Trypsin Gold Mass Spectrometry Grade, Promega) or chymotrypsin (A-chymotrypsin sequencing grade, Sigma) enzymes were used for the digestion of proteins and peptides. After digestion, peptides were extracted from gel pieces using a step-by-step extraction with a gradient of acetonitrile (15–60% acetonitrile with 1% TFA). The extraction was performed in a sonicator (Elmasonic) with ice.

Extracted peptides were desalted and concentrated with Zip-Tip C18 tips (Millipore). Both MALDI-TOF-MS and tandem ESI-MS were used to characterize the digests. The MALDI-TOF spectrometer REFLEX IV (Brüker-Daltonics) was operated in reflectron mode with an acceleration voltage of 20 kV. Samples were prepared using alpha-cyano-4-hydroxycinnamic acid as matrix. Mass spectrometer Q-TOF Micro (Waters–Micromass) was equipped with a nanoelectrospray source and coupled to 2D capillary chromatography CapLC (Waters). Chromatographic separation was achieved using 1 cm symmetry 300 Å trap column and Atlantis dC18 (75 µm × 10 cm) capillary column. Data were processed by proteomic software Mascot (MALDI) and Proteinlynx global server (LC-MS/MS). Swissprot or Uniprot databases were searched to identify protein sequences.

N-Terminal Sequencing

N-terminal amino acid sequences were determined using the Procise-Protein Sequencing System (PE Applied Biosystems, 491 Protein Sequencer, program PL PVDF Protein).

Dodecylsulfate-Polyacrylamide Gel Electrophoresis (1D-SDS-PAGE)

Electrophoresis of isolated fractions was carried out either in 20% polyacrylamide gel according to Laemmli [45] or by Tricine-SDS-PAG electrophoresis by the method of Schägger and Jagow [46] using the Mini-Protean 3 system (Biorad, USA).

Screening of Antimicrobial Activity

Antimicrobial activities of RP-HPLC-isolated fractions were determined by measuring the bacterial growth using Bioscreen C apparatus, a computer-controlled incubator evaluating turbidity of the samples (Growth Curves LtD., Finland). Turbidometric measurements were made kinetically during the course of the 24-h run. This information was processed to generate microbiological growth curves, plotting turbidity *versus* time. The testing volumes were 165 and 330 µl. Growth inhibition of the pathogens were evaluated using antimicrobial activities of fractions from the decrease in absorbance during growth curve measurements compared to growth of control microorganisms incubated without peptide. Using serial dilutions, the MIC was determined for some compounds.

The MIC is defined as the lowest final concentration of the compound at which no growth is observed during exponential phase of the bacterial growth. The test microorganisms were *E. coli* DBM 3001, *Staphylococcus aureus* DBM 3002 and *Pseudomonas aeruginosa* DBM 3081.

Solid-Phase Peptide Synthesis of β-Alanyl-Tyrosine and Analogs

The synthetic analogs of β-alanyl-tyrosine were synthesized by solid-phase methods using Fmoc/tBu strategy and 2-chlorotrityl or RinkAmide AM resin as polymeric supports. Couplings were performed using HBTU/DIPEA reagents in 1-methyl-2-pyrrolidinone (NMP). *N*-acetylation was performed with 5% acetanhydride and 1% DIPEA in NMP. All dipeptides, β-alanyl-L-tyrosine, β-alanyl-D-tyrosine, β-alanyl-L-tyrosine-NH$_2$, *N*-Ac-β-alanyl-L-tyrosine-NH$_2$, and *N*-Ac-β-alanyl-L-tyrosine were purified by RP-HPLC. The purities of the dipeptides were more than 96% as determined by analytical RP-HPLC. All dipeptides were characterized by MS. Prior to testing, the concentration of β-alanyl-tyrosine and its analogs were determined by absorption of tyrosine at 276 nm using the molar absorption coefficient $1\,420\ \text{M}^{-1}\ \text{cm}^{-1}$.

Synthesis of D-Fructopyranose-β-Alanyl-L-Tyrosine

D-fructopyranose-β-alanyl-L-tyrosine was synthesized according to Mossine *et al.* [47]. Briefly, β-alanyl-L-tyrosine (20 mg, 7.9 µmoles) and D(+)-Glucose (6 mg, 33 µmoles) were added to 10 ml of acetic acid in pyridine (1 : 1) and stirred at RT for 48 h. The reaction mixture was evaporated and the product was isolated using RP-HPLC. The identity was confirmed with MS, ^{1}H, and ^{13}C NMR.

Capillary Electrophoresis

Experimental details on capillary electrophoresis analyses and chiral separations of crude isolated β-alanyl-tyrosine, and the standards of β-alanyl-L(D)-tyrosine and its derivatives will be published elsewhere (Šolínová *et al.* manuscript in preparation).

Free-Flow Electrophoresis

Preparative electrophoretic separations were performed in a homemade free-flow electrophoretic apparatus equipped with flow-through electrophoretic chamber composed of two glass plates ($500 \times 500 \times 4$ mm) with a narrow gap (0.5 mm) between them. The chamber was thermostated from both sides by fast flowing low temperature air ($-1\,^\circ$C). The separations were performed in 0.5 M acetic acid at a flow rate of 250 ml/h, at separation voltage 3 kV, and current 125 mA. The sample flow rate was 1.6 ml/h and the residence time of the background electrolyte and sample in the chamber was 31 min. The collected fractions were evaluated by off-line UV-absorption measurements at 220 and 280 nm. Sample concentration was 30 mg/ml [48].

NMR Spectrometry

^{1}H and ^{13}C NMR spectra of compounds β-alanyl-L-tyrosine-OH and D-fructopyranose-β-alanyl-L-tyrosine were measured on a Bruker AVANCE-500 NMR spectrometer (^{1}H at 500 MHz;

Table 1 Proton and carbon-13 NMR data of compound from fraction M1b and β-D-fructopyranose-β-alanyl-L-tyrosine in D$_2$O. The NMR spectra of the pairs of native M1b (isolated) and synthetic compound were identical

Proton	^{1}H NMR β-D-Fru-β-Ala-L-Tyr-OH or M1b	Carbon	^{13}C NMR β-D-Fru-β-Ala-L-Tyr-OH or M1b
H-1a	3.30 d, $J = 12.8$	C-1	55.86
H-1b	3.24 d, $J = 12.8$	C-2	98.04
H-3	3.72 d, $J = 9.9$	C-3	72.63
H-4	3.88 dd, $J = 9.9, 3.4$	C-4	72.08
H-5	4.00 m	C-5	71.67
H-6a	4.00 m	C-6	66.79
H-6b	3.76 dd, $J = 13.1, 2.2$		
Hα1	2.73 dt, $J = 16.5, 6.6$	C=O	174.65
Hα2	2.67 dt, $J = 16.5, 6.6$	Cα	32.94
Hβ1 + Hβ2	3.27 m	Cβ	47.14
Hα	4.63 dd, $J = 9.3, 5.3$	COOH	178.24
Hβ1	3.19 dd, $J = 14.0, 5.3$	Cα	57.35
Hβ2	2.92 dd, $J = 14.0, 9.3$	Cβ	38.84
H-*ortho*	7.17 m	C-*ipso*	131.44
H-*meta*	6.86 m	C-*ortho*	133.41
		C-*meta*	118.20
		C-*para*	157.22

^{13}C at 150.9 MHz) in D$_2$O with a drop of dioxane added as an internal standard (δ_H 3.76; δ_C 69.33). Chemical shifts are given in ppm and coupling constants are given in Hz (Table 1).

RESULTS

Prophenoloxidase

Supernatant 1 (Figure 1) as well as both pellets 2 (after ammonium sulfate or acidified methanol precipitation) contained one major 75-kDa protein, as revealed by electrophoretic analysis (data not shown). Using tryptic digest and MALDI-MS, this protein was identified as prophenoloxidase, a zymogen, which is processed to phenoloxidase (EC 1.14.18.1) an enzyme involved in larval melanization [49].

Acidic Methanol Precipitation of Larvae Hemolymph

After acidified methanol precipitation, supernatant 2 was further divided into crude hydrophilic and hydrophobic fractions, using Chromabond C-18 cartridges (Figure 1 and Methods). Both fractions were analyzed and separated by RP-HPLC (Figures 2 and 3). We compared control larvae (blue lines in Figures 2 and 3) with larvae induced with bacterial suspensions of *E. coli* (red lines in Figures 2 and 3). Chromatograms obtained after induction with *P. aeruginosa* or *S. aureus* were essentially the same as the profile shown in Figure 3.
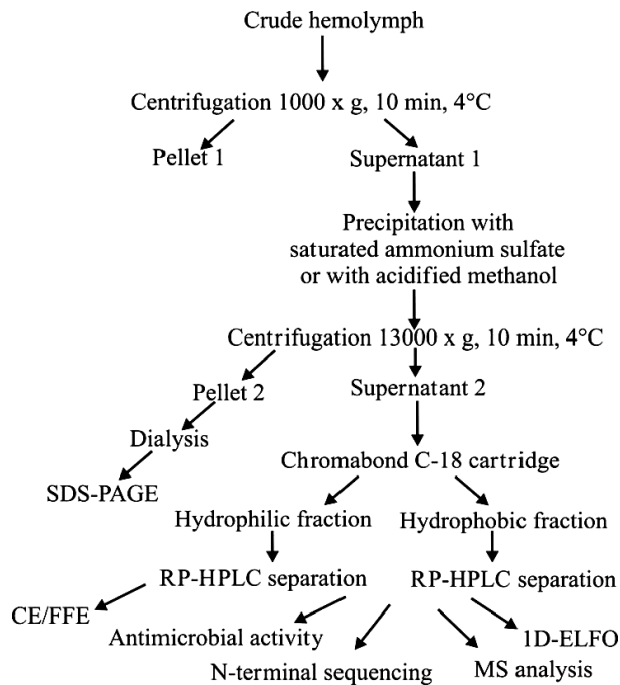
Crude hemolymph

↓

Centrifugation 1000 x g, 10 min, 4°C

Pellet 1   Supernatant 1

↓

Precipitation with
saturated ammonium sulfate
or with acidified methanol

↓

Centrifugation 13000 x g, 10 min, 4°C

Pellet 2   Supernatant 2

Dialysis

SDS-PAGE   Chromabond C-18 cartridge

Hydrophilic fraction   Hydrophobic fraction

RP-HPLC separation   RP-HPLC separation

CE/FFE

Antimicrobial activity   1D-ELFO

N-terminal sequencing   MS analysis

Figure 1 The separation of larval hemolymph.

We observed one main peak (M1, Figure 2) in the hydrophilic Chromabond C-18 fraction. In this fraction we identified dipeptide β-alanyl-tyrosine by a combination of FAB and ESI-MS/MS spectroscopy, UV-VIS spectroscopy, amino acid analysis, and NMR.

From the hydrophobic Chromabond C-18 fraction we isolated different peaks, marked as M1–M19, from which fractions M13–M15 were found only in larvae induced with the bacterial suspension of *E. coli* (Figure 3). Fractions M1–M19 were further analyzed by gel electrophoresis (Figure 4) and this analysis revealed the presence of different peptides and proteins of relatively low molecular masses in fractions M7–M19.
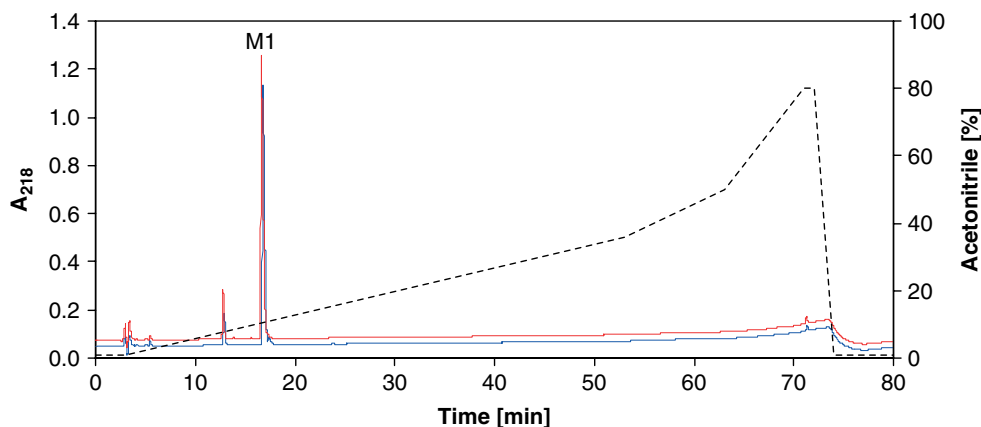
Ammonium Sulfate Precipitation of Larvae Hemolymph

The hydrophilic Chromabond C-18 fraction obtained from supernatant 2 after ammonium sulfate precipitation of hemolymph contained only salts. The RP-HPLC analysis of the hydrophobic Chromabond C-18 fraction is shown in Figure 5. We found no difference in HPLC profiles between induced and noninduced larvae. The isolated peaks were further analyzed by gel electrophoresis (Figure 6) and this analysis revealed different proteins in fractions S3–S9. Fractions S3, S4, S6, and S7 contained essentially pure proteins while fractions S5 and S9 were composed of several proteins.

Antimicrobial Activity

All isolated fractions, M1–M19 and S1–S9, were tested for their antimicrobial activity against *E. coli*, *P. aeruginosa* (Gram-negative bacteria) and *S. aureus* (Gram-positive bacteria) at concentrations up to 1 mg/ml. Some fractions displayed antimicrobial activities.

Among fractions M1–M19, only fractions M13–M15 have shown significant antimicrobial activity. Fraction M13 completely inhibited the growth of *P. aeruginosa* at a concentration 970 µg/ml as shown in Figure 7(A). Fractions M14 and M15 effectively inhibited *S. aureus* growth at concentrations 100 µg/ml and 400 µg/ml, respectively (Figure 7(B)).

Among fractions S1–S9, only S4 and S7 have shown any antimicrobial activity. Fractions S4 and S7 significantly inhibited growth of *S. aureus*, but only slightly inhibited growth of *E. coli* (Figure 8). The MIC of fraction S4 was determined to be between 80 and 115 µg/ml for *S. aureus*.

β-Alanyl-Tyrosine

As mentioned above, we observed one main peak (M1, Figure 2) in the hydrophilic Chromabond C-18 fraction
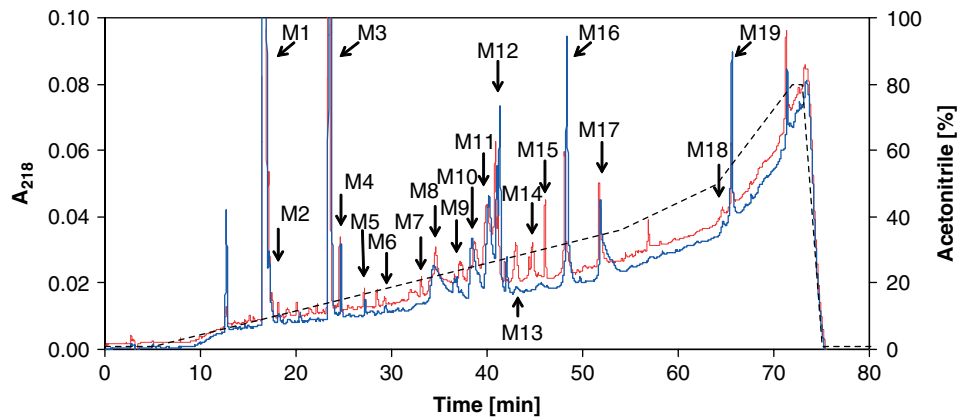

Figure 2 RP-HPLC analysis of Chromabond C-18 hydrophilic fraction from *S. bullata* hemolymph obtained after precipitation with acidified methanol. Chromatogram of control larvae is shown in blue and of induced larvae is shown in red. The peak of β-alanyl-tyrosine is marked by M1.

Figure 3 RP-HPLC analysis of Chromabond C-18 hydrophobic fraction from *S. bullata* hemolymph obtained after precipitation with acidified methanol. Chromatogram of control larvae is shown in blue and of induced larvae is shown in red. The isolated peaks are marked as M1–M19.
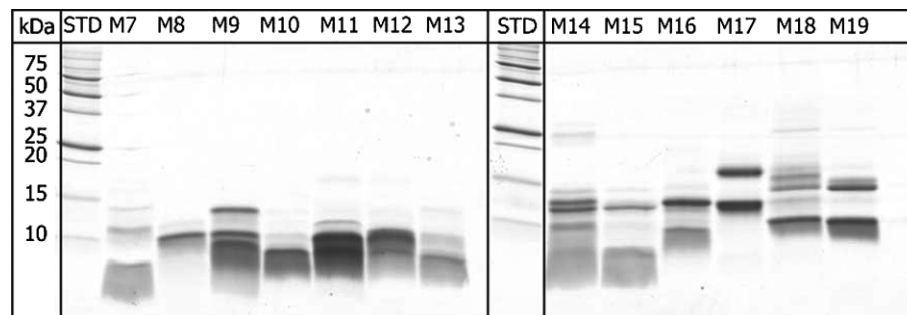

Figure 4 SDS-PAGE of HPLC-isolated fractions M7–M19 obtained after precipitation with acidified methanol.
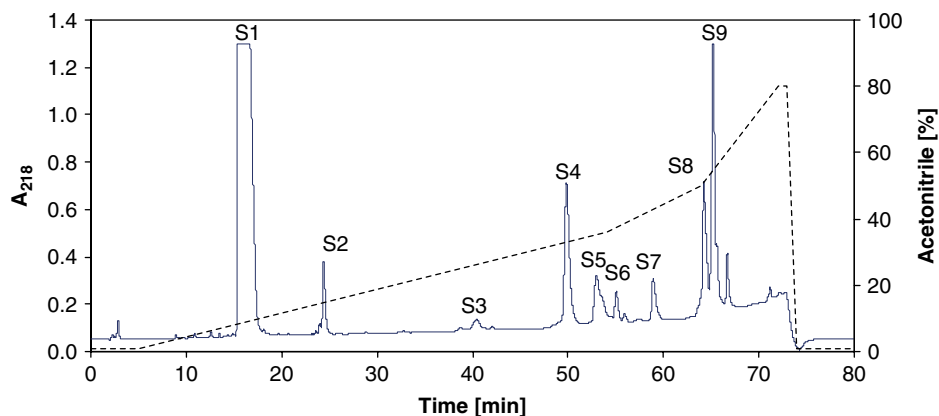

Figure 5 RP-HPLC analysis of Chromabond C-18 hydrophobic fraction of *S. bullata* hemolymph obtained after precipitation with ammonium sulfate. The isolated peaks are marked as S1–S9. Chromatograms from induced and control larvae were essentially the same.

obtained after precipitation of hemolymph with acidified methanol. The compound was identified as dipeptide β-alanyl-tyrosine. The structure was determined by ^{1}H and ^{13}C NMR spectra. Proton and carbon signals were structurally assigned by means of the series of 1D- (^{1}H, ^{13}C-APT) and 2D-NMR spectra (^{1}H,^{1}H-COSY, ^{1}H,^{13}C-HMQC, ^{1}H,^{13}C-HMBC). We also synthesized β-alanyl-tyrosine using solid-phase synthesis and found

the NMR spectra of the pairs of native and synthetic compounds to be identical (data not shown).

Using capillary electrophoresis with a cyclodextrin-based chiral pseudo stationary phase, we proved that tyrosine in the isolated β-alanyl-tyrosine is present in its L-form (Šolínová *et al.* manuscript in preparation). Interestingly, capillary electrophoresis also revealed that fraction M1 contains an admixture
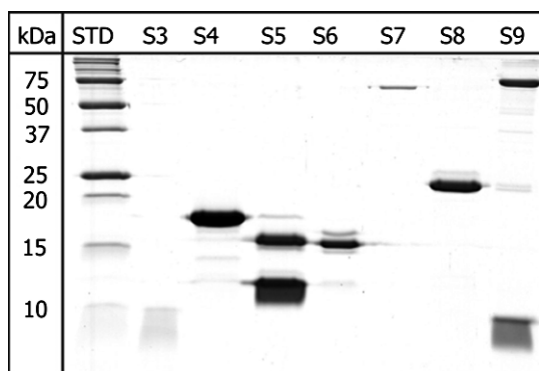
Figure 6 SDS-PAGE of RP-HPLC-isolated fractions S3–S9 obtained after precipitation with ammonium sulfate.
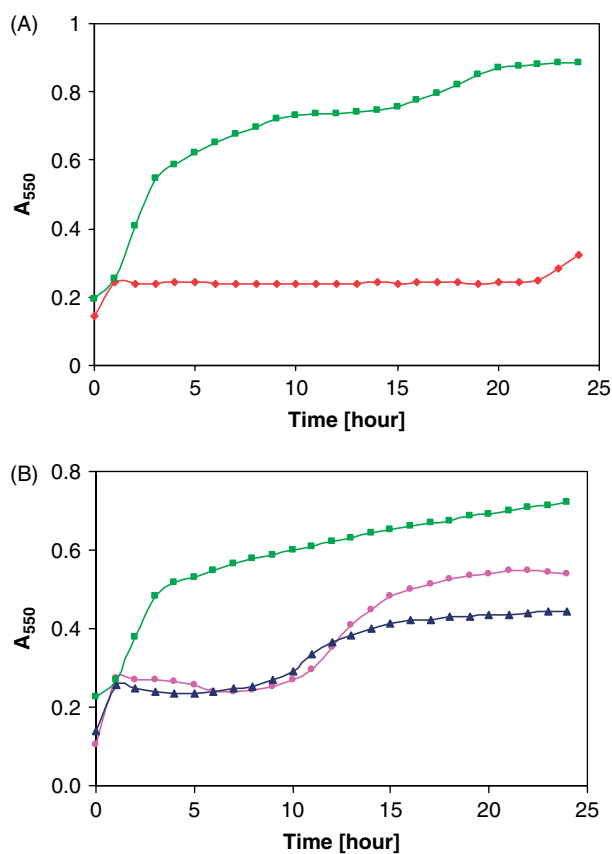

Figure 7 (A) Inhibition of *Pseudomonas aeruginosa* growth by fraction M13 at 970 µg/ml (♦). The control growth of *Pseudomonas aeruginosa* is displayed as ■. B. Inhibition of Staphylococcus *aureus* growth by fraction M14 at 400 µg/ml (●) and fraction M15 at 100 µg/ml (▲). The control growth of Staphylococcus *aureus* is displayed as ■.

Figure 8 Dose-dependent inhibition of bacterial growth of *Staphylococcus aureus* (red) and *Escherichia coli* (blue) by fractions S4 (Figure 8(A)) and S7 (Figure 8(B)).

(about 1–3%). This admixture was not detectable in the M1 fraction using ^{1}H or ^{13}C NMR. The admixture was highly enriched using free-flow electrophoresis (FFE), (see Methods, data not shown) and the FFE prepurified fraction was further separated using RP-HPLC (Figure 9). We isolated two compounds, M1a
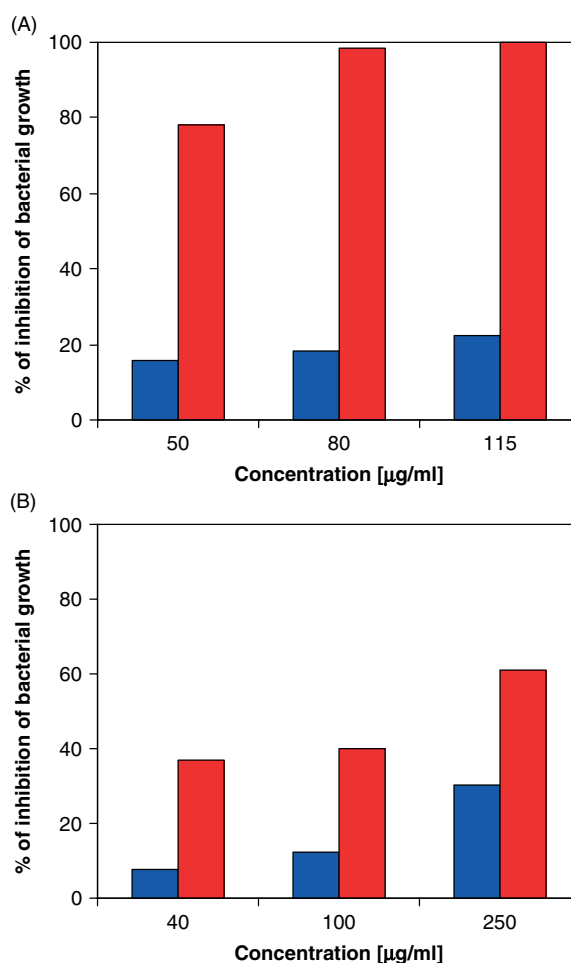
and M1b. Using MS we found that fraction M1a is β-alanyl-tyrosine (Mr 252.11) and that fraction M1b is a compound with a higher Mr (414.28). The structure of the compound in fraction M1b was determined by ^{1}H and ^{13}C NMR spectra. Proton and carbon NMR data are summarized in Table 1. We concluded that fraction M1b is, with a high probability, β-alanyl-L-tyrosine with D-fructose attached to its *N*-terminus (β-D-fructopyranose-β-alanyl-L-tyrosine, see Figure 10). We also synthesized this compound using Amadori rearrangement [47] (see Methods) and found the NMR spectra of the native and synthetic pairs were identical.

Dipeptide β-alanyl-tyrosine has already been identified in *Neobellieria (Sarcophaga) bullata* by Meylaers *et al.* [20]. The authors found that this compound displays antimicrobial activity in the range 8–30 mM. For this reason we decided to test the antimicrobial activity of fraction M1, synthetic β-alanyl-L-tyrosine and several synthetic analogs at higher concentrations then 1 mg/ml (4 mM). Fraction M1b and synthetic β-D-fructose-β-alanyl-L-tyrosine were also tested for their
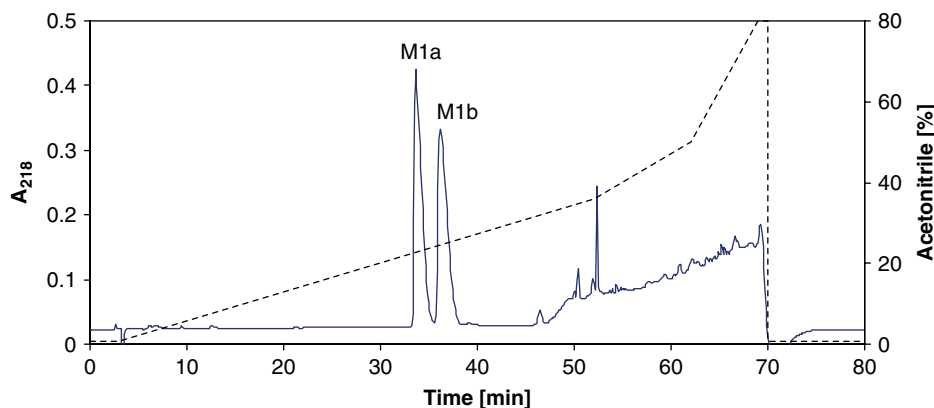
Figure 9 RP-HPLC separation of FFE-prepurified fraction M1. Injection of 30 μg of crude material. The isolated peaks are marked as M1a and M1b. For details, see Methods.

antimicrobial activity. All compounds together with their antimicrobial activities are listed in Table 2.

We succeeded in determining the MIC for some of the β-alanyl-tyrosine derivatives against *E. coli, S. aureus,* and *P. aeruginosa.* Fraction M1, a mixture of M1a and M1b, inhibited microorganisms with MIC in the range of 10–15 mM. Interestingly, synthetic β-alanyl-L-tyrosine-OH was more active against all microorganisms than fraction M1 as wells as synthetic β- alanyl-D-tyrosine-OH. Acetylation of the *N*-terminus of β-alanyl-L-tyrosine-OH had a slightly negative effect
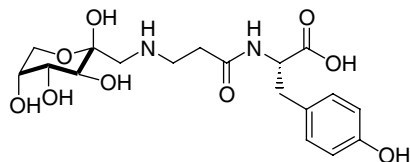
on the antimicrobial activity compared to β-alanyl-L-tyrosine-OH. Amidation of the *C*-terminus resulted in the loss of activity of respective derivatives *N*-Ac-β-alanyl-L-tyrosine-OH and *N*-Ac-β-alanyl-L-tyrosine-NH$_2$. Isolated (M1b) and synthetic D-fructopyranose-β-alanyl-L-tyrosine-OH were inactive at the highest dose used (5 mM).

Characterization of Active Protein and Peptide Fractions

Active protein and peptide fractions S4, S7, and M13–M15 were further analyzed by MALDI-TOF-MS and ESI-TOF-MS to determine the exact relative molecular weights of the respective peptides and proteins. The data are summarized in Table 3 and are compared with the data obtained from gel electrophoresis.

Antimicrobially active protein and peptide fractions were further characterized to identify respective peptides and proteins. Protein spots were excised from SDS gels, digested by trypsin or chymotrypsin, and analyzed by MALDI-MS. Alternatively, proteins were submitted to the *N*-terminal sequencing after electroblotting into PVDF membrane. The resulting peptide sequences were analyzed by searching available protein databases (Swissprot or Uniprot). Results are shown in Table 4.

The sequence of protein in fraction S4 revealed about 50% identity with odorant-binding protein 99b (OBP99b) from *Drosophila melanogaster*. The protein in fraction S7 was identified as transferrin both by enzymatic digests/MALDI-MS and by *N*-terminal sequencing. Comparing the obtained sequence with available protein databases did not allow identifying peptide(s) from fraction M13. The sequence of peptide in fraction M15 is almost identical to the sequence of antimicrobial peptide sapecin from *S. peregrina*. The same is true for the short sequence of peptide in fraction M14. The results obtained from *N*-terminal sequencing of fractions M14 and M15 were confirmed by MALDI-MS analysis of chymotryptic digests.

Figure 10 Structure of β-D-fructopyranose-β-alanyl-L-tyrosine.

Table 2 Antimicrobial activities of β-alanyl-tyrosine and its analogues. The MIC is defined as the lowest final concentration of the compound, at which no growth is observed during exponential phase of the bacteria growth. NI means no inhibition at 5 mM concentration

Compound	MIC (mM)		
	E. coli	*S. aureus*	*P. aeruginosa*
M1	10	15	15
β-Ala-L-Tyr-OH	6	7.5	6
β-Ala-D-Tyr-OH	8.5	15	15
N-Ac-β-Ala-L-Tyr-OH	8.5	8.5	8.5
N-Ac-β-Ala-L-Tyr-NH$_2$	>20	>20	>20
β-Ala-L-Tyr-NH$_2$	≫20	≫20	≫20
M1b	NI	NI	NI
D-fructopyranose-β-Ala-L-Tyr-OH	NI	NI	NI

Table 3 Determination of relative molecular weight (Mr) of peptides and proteins by direct mass spectrometry analysis or by SDS gel electrophoresis. $Mr_{Tris-PAGE}$ or $Mr_{Tricine-PAGE}$ means that the SDS-electrophoresis was performed in Tris or Tricine-buffered system, respectively

Fraction name	$Mr_{Tris-PAGE}$	$Mr_{Tricine-PAGE}$	Mr_{ESI-MS}	$Mr_{MALDI-MS}$
S4	19 000	—	16 783	16 777
S7	69 000	—	69 097	69 549
M13	10 000	10 000, 6000	4808, 3498	4813
M14	12 000, 5000	10 000, 4000	3754	3714, 9632
M15	12 000, 5000	10 000, 4000	4060	4060, 9630

Table 4 Identification of active protein fractions by *N*-terminal sequencing or MALDI-MS of tryptic digests

Fraction	N-terminal sequencing		Tryptic digest MS/NP/SC	Chymotryptic digest MS/NP/SC
S4	DHHEGHHEHHEHDTXEYVVKTQQDLVKYRE DXGAKLXVSXELMXKYKNNE	OBP99b	Unidentified	Unidentified
S7	EEQTYMCV	Transferrin	Transferrin 84/9/12	Transferrin 72/16/22
M13	AIAMARSN	Unidentified	Unidentified	Unidentified
M14	ATXDLLSG	Sapecin	Unidentified	Unidentified
M15	ATXDLLSGTGINHSAXAAHXLLRGNRGGY XNGKGVXVXRN	Sapecin	Unidentified	Sapecin 69/3/72

MS, Mascot score; NP, number of peptides assigned; SC, sequence coverage in %

DISCUSSION

We attempted to isolate and identify new antimicrobial compounds from hemolymph of larvae of *Sarcophaga bullata*, which is in some studies, assigned as *Neobellieria bullata*. However, both names belong to the same fleshfly species. We used third-instar larvae in their wandering period. The larvae were injected with bacterial suspensions of *E. coli* or pricked by an entomological needle to induce an immune response and production of antimicrobial compounds. The induction of larvae with other bacteria gave very similar results.

Supernatant 1 (Figure 1) as well as both pellets 2 (after ammonium sulfate or acidified methanol precipitation) contained one major 75-kDa protein as revealed by electrophoretic analysis (data not shown). We identified this protein as prophenoloxidase, a zymogen, which is processed to phenoloxidase (EC 1.14.18.1). This result shows that prophenoloxidase is a major protein in *S. bullata* larvae hemolymph. The most immediate immune response within minutes is the activation of the prophenoloxidase-activating enzyme that converts prophenoloxidase to phenoloxidase [33]. Phenoloxidase is an enzyme involved in melanin biosynthesis and is also important in cuticular sclerotization, wound healing, and in the encapsulation of foreign material [49].

We did not detect any antimicrobial activity of prophenoloxidase in our study.

Using C-18 cartridges, supernatants 2 were separated into hydrophilic and hydrophobic fractions. The hydrophilic fraction obtained after precipitation with acidified methanol contained one major compound (peak M1, Figure 2), which was identified as dipeptide β-alanyl-L-tyrosine. The hydrophilic fraction obtained after ammonium sulfate precipitation contained a high concentration of salts and was not further analyzed. However, it is highly probable that this fraction also contained β-alanyl-L-tyrosine as a major component. Both hydrophobic fractions also contained a major peak with a short retention time, M1 or S1 as shown in Figures 2 and 4, respectively. We again identified dipeptide β-alanyl-L-tyrosine in both peaks M1 and S1.

Considering the above-described results, it is clear that major peptide/protein components in *S. bullata* hemolymph are enzyme prophenoloxidase and dipeptide β-alanyl-L-tyrosine. Both these two compounds have an important role in larvae melanization [49]. Other roles, especially in larvae antimicrobial defense, will be discussed later.

On the other hand, regardless of the fact that chromatograms shown in Figures 2 and 4 both have major peaks M1 and S1 (β-alanyl-L-tyrosine), they

differ significantly in other peaks. Figure 4 shows that fractions M7–M19 contain peptides or small proteins of Mr about 3–15 kDa. Among fractions S3–S9 we found proteins of higher Mr in S4, S7, and S9 (15–75 kDa). It means that acidified methanol treatment does not precipitate smaller proteins from hemolymph and that ammonium sulfate precipitation (saturation to 70%) allows detection of larger proteins in the supernatant. Both precipitation protocols are thus complementary and enable detection of different proteins or peptides.

We identified dipeptide β-alanyl-L-tyrosine in fractions M1 and S1. Its structure was confirmed by MS, ^{1}H and ^{13}C NMR and the L-form of tyrosine by capillary electrophoresis using chiral selectors. This compound has previously been found in *S. (N.) bullata* by Levenbook *et al.* [50] and Meylaers *et al.* [20]. Levenbook *et al.* also proposed that tyrosine is present in its L-form by comparing specific rotation with the synthetic dipeptide. β-Alanyl-tyrosine is known to cause paralysis in adult insects but it is not toxic for larvae where its concentration changes significantly during development with highest levels (around 20 mM) reached just before puparization [51,52]. The role of this dipeptide in larvae melanization and puparization is highly probable [50,53] and is in agreement with our finding that prophenoloxidase and β-alanyl-L-tyrosine are the most abundant species in the hemolymph of third-instar larvae of *S. bullata* in the wandering period.

Meylaers *et al.* [20] detected an antimicrobial activity of β-alanyl-tyrosine against various bacteria at 8–30 mM concentration range. They also prepared several inactive analogs of this compound. In our study, we found β-alanyl-L-tyrosine slightly more active (MICs in the range of 6–15 mM) than Meylaers *et al.* [20]. The reason for this difference may be due to the sensitivity of microorganisms or the high hygroscopicity of the dipeptide. This is why we determined the concentration of β-alanyl-tyrosine and its analogs based on the absorption of tyrosine (see methods). In the course of capillary electrophoresis analyses of fraction M1 we found an admixture, which was then identified as β-D-fructopyranose-β-alanyl-L-tyrosine. We have not detected any antimicrobial activity of this compound in our experiments. This may explain the somewhat weaker potency of fraction M1 to inhibit bacterial growth compared to synthetic β-alanyl-L-tyrosine. We tested fraction M1b and synthetic β-D-fructopyranose-β-alanyl-L-tyrosine only up to 5 mM concentration (2.25 mg/ml). To achieve a higher concentration it would be necessary to isolate more of the compounds, which is difficult to achieve due to the laborious and difficult separation of fractions M1a and M1b (Figure 9). This was also the case of synthetic β-D-fructopyranose-β-alanyl-L-tyrosine because the reaction (see Methods) results in the 1 : 1 equilibrium of β-alanyl-L-tyrosine and the product. Concerning other β-alanyl-L-tyrosine analogs, we can observe a slightly negative effect

of *N*-acetylation and a highly negative effect of the *C*-terminus amidation. L-Tyrosine is more favorable for antimicrobial activity of β-alanyl-tyrosine than D-tyrosine. We agree with Meylaers *et al.* [20] that a weak antimicrobial activity of β-alanyl-L-tyrosine could have physiological relevance due to its high concentration in larvae hemolymph (20 mM according to Levenbook *et al.* [50]). β-D-fructopyranose-β-alanyl-L-tyrosine can be a reaction product of highly abundant β-alanyl-L-tyrosine with D-glucose, which is certainly present in larvae bred on beef liver. Both compounds readily react following Amadori rearrangement [47]. It is also possible that β-D-fructopyranose-β-alanyl-L-tyrosine can possess antimicrobial effect or other roles against other microorganisms than tested in this study.

Among all isolated fractions, only fractions M13–M15 and fractions S4 and S7 displayed antimicrobial activity below 1 mg/ml. We were not able to determine MICs for all fractions against tested microorganisms due to the difficulty of isolating sufficient amounts of the material.

Proteins in fractions S4 and S7 inhibited the growth of *S. aureus* more potently than the growth of *E. coli* (Figure 8). We can conclude from the available data that the MIC of fraction S4 against *S. aureus* is between 80 and 115 µg/ml. Active protein in fraction S4 has been partially characterized. The 50 amino acid *N*-terminal sequence of this 16-kDa reveals about 50% sequence identity to odorant-binding protein 99b (OBP99b, *CG7592-PA*) from *D. melanogaster*. It is probable that protein S4 is a *S. bullata* homologue of *Drosophila's* OBP99b. The difference in the *N*-terminal sequence may be due to the low homology between *Drosophila* and *S. bullata* proteins. To further substantiate the identification of this potential *S. bullata* OBP99b we amplified the cDNA sequence of the 'potential' gene with PCR using a degenerated primer designed according to the *N*-terminal amino acid sequence of protein S4 (Table 3). PCR amplicon approximately 500 bp long was isolated and sequenced. However, only partial nucleotide sequence was readable (data not shown). Comparing the obtained sequence with *Drosophila* nucleotide sequences has not revealed any significant homology. Further experiments to identify the respective gene are in course.

OBPs are abundant, small, soluble proteins that are believed to participate in odor detection by facilitating or restricting access of the odorant to the receptors. There are 51 OBP genes in *Drosophila* [54]. We have not found any report concerning antimicrobial activity of odorant-binding proteins. Levy *et al.* [55] showed that OBP99c in *Drosophila* was specifically over-expressed after fungal infection but repressed after bacterial infection. In our study we did not found any significant induction of protein S4 after bacterial induction of larvae. Chromatograms from induced and noninduced larvae were essentially the same (Figure 5). It will be interesting to produce higher quantity of recombinant

OBP99b and to investigate its antimicrobial activity and mode of action more in detail using different methods and microorganisms.

Protein in fraction S7 was identified as transferrin by *N*-terminal sequencing and MS analysis of tryptic digest. Tranferrin is involved in the immune response of vertebrates and invertebrates [56,57]. It can inhibit bacterial growth by reducing free iron levels [58]. If we consider that both fractions S4 (probably *S. bullata* OBP99b) and S7 (transferrin) consisted of pure proteins of 16 and 70 kDa, respectively, the inhibition of bacterial growth as displayed in Figure 8 was achieved at low micromolar concentrations.

Fraction M13 inhibited the growth of *P. aeruginosa* but not the growth of *E. coli.* It seems that fraction M13 has bactericidal antibacterial effect against *P. aeruginosa* with an MIC value lower than 1 mg/ml (Figure 7(A)). The basis for the different susceptibilities of bacterial species against particular peptides is not clear [2]. One hypothesis that explains different bacterial sensitivities to antimicrobial peptides is due to the different lipopolysaccharide composition in the outer membranes of bacteria or different resistance mechanisms [25]. We have not succeeded in identifying the peptide in fraction M13 either by *N*-terminal sequencing or by tryptic or chymotryptic digests. The identification was complicated with low amount of isolated material.

Using *N*-terminal sequencing, we determined the entire amino acid sequence (40 amino acids) of peptide in fraction M15, but we succeeded in determining only ten *N*-terminal amino acids in fraction M14. Provided that cysteines are in positions X (Table 4), the sequence of peptide M15 almost completely matches with *S. peregrina* sapecin [59]. The only difference is in the position 34 (G for *S. bullata* and A for *S. peregrina*). We suppose that active peptide M15 is a *S. bullata* homologue of *S. peregrina* antimicrobial peptide sapecin. The theoretical relative molecular weight (Mr) of peptide M15 is 4060 (provided that X residues are cysteines forming disulfide bridges, Table 4) and is in perfect agreement with the experimental value 4060 obtained with ESI/MALDI-MS (Table 3). In the case of fraction M14, we found signals 3754 (ESI-MS) and 3714 (MALDI-MS), which match neither with the Mr of peptide M15 shortened by two or by three amino acids nor with sapecin C from *S. peregrina* [60] and its possible fragments. We also performed MS-MS analysis of fraction M14 to determine if this peptide is or is not *N*-terminal fragment of peptide M15 or other sapecin, but these experiments were not successful.

Sapecin, which consists of 40 amino acids, is an insect defensin and can inhibit the growth of G+ bacteria. Sapecin is the first identified defensin in *S. peregrina* and was isolated from the embryonic cell line NIH-Sape-4 by Matsuyama and Natori [61]. Both fractions M14 and M15 inhibited the growth of *S.*

aureus, which is in agreement with the data of Yamada and Natori [62]. Peptide in fraction M14 displays lower antibacterial potency than peptide M15 (Figure 7(B)) and it is not excluded that the peptide in M14 is a *S. bullata* homologue of *S. peregrina* sapecin C [60] or its fragment.

In M1–M19, obtained after acidic methanol precipitation, we detected the induction of fractions M13–M15 (Figure 3). However, we have not detected the induction of any of fractions S1–S9 obtained after ammonium sulfate precipitation (Figure 5). Using RT-qPCR technique we confirmed the massive induction of sapecin (M15 and M14) and also a moderate induction of tranferrin (S7) (unpublished results, manuscript in preparation).

Insect immune response is a complicated process. Antimicrobial peptides frequently act synergistically; some proteins have transporter functions; peptide inhibitors can block processing enzymes involved in activating cascades or different enzymes can activate antimicrobially active proteins or peptides. In this study we presented two different isolation protocols, which resulted in the identification of several already known and two novel antimicrobial proteins or peptides from the hemolymph of fleshfly *S. bullata*. We hope that our study will shed more light into the complicated process of immune response in *S. bullata* larvae.

REFERENCES

1. Bulet P, Stocklin R, Menin L. Anti-microbial peptides: from invertebrates to vertebrates. *Immunol. Rev.* 2004; **198**: 169–184.
2. Zasloff M. Antimicrobial peptides of multicellular organisms. *Nature* 2002; **415**: 389–395.
3. Hancock REW. Peptide antibiotics. *Lancet* 1997; **349**: 418–422.
4. Vizioli J, Salzet M. Antimicrobial peptides from animals: focus on invertebrates. *Trends Pharmacol. Sci.* 2002; **23**: 494–496.
5. Boman HG. Antibacterial peptides: basic facts and emerging concepts. *J. Int. Med.* 2003; **254**: 197–215.
6. Ryge TS, Hansen PR. Novel lysine-peptoid hybrids with antibacterial properties. *J. Pept. Sci.* 2005; **11**: 727–734.
7. Tossi A. AMPs database, 2007; http://www.bbcm.univ.trieste.it/~tossi/amsdb.html.
8. Steiner H, Hultmark D, Engstrom A, Bennich H, Boman HG. Sequence and specificity of two antibacterial proteins involved in insect immunity. *Nature* 1981; **292**: 246–248.

9. Dimarcq JL, Bulet P, Hetru C, Hoffmann J. Cysteine-rich antimicrobial peptides in invertebrates. *Biopolymers* 1998; **47**: 465–477.

10. Okada M, Natori S. Purification and characterization of an antibacterial protein from haemolymph of Sarcophaga peregrina (flesh-fly) larvae. *Biochem. J.* 1983; **211**: 727–734.

11. Yamauchi H. Two novel insect defensins from larvae of the cupreous chafer, *Anomala cuprea*: purification, amino acid sequences and antibacterial activity. *Insect Biochem. Mol. Biol.* 2001; **32**: 75–84.

12. Gobbo M, Biondi L, Filira F, Gennaro R, Benincasa M, Scolaro B, Rocchi R. Antimicrobial peptides: synthesis and antibacterial activity of linear and cyclic drosocin and apidaecin 1b analogues. *J. Med. Chem.* 2002; **45**: 4494–4504.

13. Bulet P, Dimarcq JL, Hetru C, Lagueux M, Charlet M, Hegy G, Vandorsselaer A, Hoffmann JA. A novel inducible antibacterial peptide of *Drosophila* carries an *O*-glycosylated substitution. *J. Biol. Chem.* 1993; **268**: 14893–14897.

14. Otvos L. The short proline-rich antibacterial peptide family. *Cell. Mol. Life Sci.* 2002; **59**: 1138–1150.

15. Goumon Y, Lugardon K, Gadroy P, Strub JM, Welters ID, Stefano GB, Aunis D, Metz-Boutigue MH. Processing of proenkephalin-A in bovine chromaffin cells. Identification of natural derived fragments by *N*-terminal sequencing and matrix-assisted laser desorption ionization-time of flight mass spectrometry. *J. Biol. Chem.* 2000; **275**: 38355–38362.

16. Salzet M. Vertebrate innate immunity resembles a mosaic of invertebrate immune responses. *Trends Immunol.* 2001; **22**: 285–288.

17. Brogden KA, De Lucca AJ, Bland J, Elliott S. Isolation of an ovine pulmonary surfactant-associated anionic peptide bactericidal for *Pasteurella haemolytica*. *Proc. Natl. Acad. Sci. U.S.A.* 1996; **93**: 412–416.

18. Leem JY, Nishimura C, Kurata S, Shimada I, Kobayashi A, Natori S. Purification and characterization of *N*-beta-alanyl-5-S-glutathionyl-3,4-dihydroxyphenylalanine, a novel antibacterial substance of Sarcophaga peregrina (flesh fly). *J. Biol. Chem.* 1996; **271**: 13573–13577.

19. Leem JY, Jeong IJ, Park KT, Park HY. Isolation of p-hydroxycinnamaldehyde as an antibacterial substance from the saw fly, *Acantholyda parki, S. FEBS Lett.* 1999; **442**: 53–56.

20. Meylaers K, Cerstiaens A, Vierstraete E, Baggerman G, Michiels CW, De Loof A, Schoofs L. Antimicrobial compounds of low molecular mass are constitutively present in insects: characterisation of beta-alanyl-tyrosine. *Curr. Pharm. Des.* 2003; **9**: 159–174.

21. Fogaca AC, da Silva PI, Miranda MTM, Bianchi AG, Miranda A, Ribolla PEM, Daffre S. Antimicrobial activity of a bovine hemoglobin fragment in the tick *Boophilus microplus*. *J. Biol. Chem.* 1999; **274**: 25330–25334.

22. Huang HW. Action of antimicrobial peptides: two-state model. *Biochemistry* 2000; **39**: 8347–8352.

23. Shai Y. Mechanism of the binding, insertion and destabilization of phospholipid bilayer membranes by alpha-helical antimicrobial and cell non-selective membrane-lytic peptides. *Biochim. Biophys. Acta Biomembr.* 1999; **1462**: 55–70.

24. Silvestro L, Weiser JN, Axelsen PH. Antibacterial and antimembrane activities of cecropin A in *Escherichia coli*. *Antimicrob. Agents Chemother.* 2000; **44**: 602–607.

25. Yeaman MR, Yount NY. Mechanisms of antimicrobial peptide action and resistance. *Pharmacol. Rev.* 2003; **55**: 27–55.

26. Kragol G, Lovas S, Varadi G, Condie BA, Hoffmann R, Otvos L. The antibacterial peptide pyrrhocoricin inhibits the ATPase actions of DnaK and prevents chaperone-assisted protein folding. *Biochemistry* 2001; **40**: 3016–3026.

27. Otvos LOI, Rogers ME, Consolvo PJ, Condie BA, Lovas S, Bulet P, Blaszczyk-Thurin M. Interaction between heat shock proteins and antimicrobial peptides. *Biochemistry* 2000; **39**: 14150–14159.

28. Basak A, Ernst B, Brewer D, Seidah NG, Munzer JS, Lazure C, Lajoie GA. Histidine-rich human salivary peptides are inhibitors of proprotein convertases furin and PC7 but act as substrates for PC1. *J. Pept. Res.* 1997; **49**: 596–603.

29. Verbanac D, Zanetti M, Romeo D. Chemotactic and protease-inhibiting activities of antibiotic peptide precursors. *FEBS Lett.* 1993; **317**: 255–258.

30. Yan H, Hancock RE. Synergistic interactions between mammalian antimicrobial defense peptides. *Antimicrob. Agents Chemother.* 2001; **45**: 1558–1560.

31. Dimarcq JL, Hunneyball I. Pharma-entomology: when bugs become drugs. *Drug Discov. Today* 2003; **8**: 107–110.

32. Otvos L. Antibacterial peptides isolated from insects. *J. Pept. Sci.* 2000; **6**: 497–511.

33. Royet J. Infectious non-self recognition in invertebrates: lessons from Drosophila and other insect models. *Mol. Immunol.* 2004; **41**: 1063–1075.

34. Chase MR, Raina K, Bruno J, Sugumaran M. Purification, characterization and molecular cloning of prophenoloxidases from *Sarcophaga bullata*. *Insect Biochem. Mol. Biol.* 2000; **30**: 953–967.

35. Leclerc V, Pelte N, Chamy LE, Martinelli C, Ligoxygakis P, Hoffmann JA, Reichhart JM. Prophenoloxidase activation is not required for survival to microbial infections in *Drosophila*. *EMBO Rep.* 2006; **7**: 231–235.

36. Vilmos P, Kurucz E. Insect immunity: evolutionary roots of the mammalian innate immune system. *Immunol. Lett.* 1998; **62**: 59–66.

37. Iwanaga S, Lee BL. Recent advances in the innate immunity of invertebrate animals. *J. Biochem. Mol. Biol.* 2005; **38**: 128–150.

38. Hoffmann JA, Reichhart JM. *Drosophila* innate immunity: an evolutionary perspective. *Nature Immunol.* 2002; **3**: 121–126.

39. Hultmark D. *Drosophila* immunity: paths and patterns. *Curr. Opin. Immunol.* 2003; **15**: 12–19.

40. Tzou P, De Gregorio E, Lemaitre B. How Drosophila combats microbial infection: a model to study innate immunity and host-pathogen interactions. *Curr. Opin. Microbiol.* 2002; **5**: 102–110.

41. Leclerc V, Reichhart JM. The immune response of *Drosophila melanogaster*. *Immunol. Rev.* 2004; **198**: 59–71.

42. Fraenkel G. Molting and development in undersized fly larvae. In *The Insect Integument*, Hepburn AR (ed.). Elsevier: Amsterdam, 1976; 323–338.

43. Lemaitre B, Hoffmann J. The host defense of Drosophila melanogaster. *Annu. Rev. Immunol.* 2007; **25**: 697–743.

44. Zdarek J. Endocrine control of the pupariation behavior in flies. *Gen. Comp. Endocrinol.* 1980; **40**: 361–361.

45. Laemmli UK. Cleavage of structural proteins during the assembly of the head of bacteriophage T4. *Nature* 1970; **227**: 680–685.

46. Schagger H, von Jagow G. Tricine-sodium dodecyl sulfate-polyacrylamide gel electrophoresis for the separation of proteins in the range from 1 to 100 kDa. *Anal. Biochem.* 1987; **166**: 368–379.

47. Mossine VV, Glinsky GV, Feather MS. The preparation and characterization of some Amadori compounds (1-amino-1-deoxy-D-fructose derivatives) derived from a series of aliphatic omega-amino acids. *Carbohydr. Res.* 1994; **262**: 257–270.

48. Kasicka V, Prusik Z, Sazelova P, Jiracek J, Barth T. Theory of the correlation between capillary and free-flow zone electrophoresis and its use for the conversion of analytical capillary separations to continuous free-flow preparative processes. Application to analysis and preparation of fragments of insulin. *J. Chromatogr., A* 1998; **796**: 211–220.

49. Sugumaran M. Comparative biochemistry of eumelanogenesis and the protective roles of phenoloxidase and melanin in insects. *Pigment Cell Res.* 2002; **15**: 2–9.

50. Levenbook L, Bodnaryk RP, Spande TF. Beta-alanyl-L-tyrosine. Chemical synthesis, properties and occurrence in larvae of the fleshfly *Sarcophaga bullata* Parker. *Biochem. J.* 1969; **118**: 837–841.

51. Chiou SJ, Cerstiaens A, Kotanen SP, De Loof A, Schoofs L. Insect larvae contain substances toxic to adults: the discovery of paralysins. *J. Insect Physiol.* 1998; **44**: 405–411.

52. Chiou SJ, Kotanen S, Cerstiaens A, Daloze D, Pasteels JM, Lesage A, Drijfhout JW, Verhaert P, Dillen L, Claeys M, De MH, Nuttin B, De LA, Schoofs L. Purification of toxic compounds from larvae of the gray fleshfly: the identification of paralysins. *Biochem. Biophys. Res. Commun.* 1998; **246**: 457–462.

53. Dunn PE, Fader RG, Regnie FE. Metabolism of beta-Alanyl-L-Tyrosine in *Sarcophaga bulllata*. *J. Insect Physiol.* 1977; **23**: 1021–1029.

54. Hekmat-Scafe DS, Scafe CR, Mckinney AJ, Tanouye MA. Genome-wide analysis of the odorant-binding protein gene family in *Drosophila melanogaster*. *Cold Spring Harbor Lab. Press* 2002; **12**: 1357–1369.

55. Levy F, Bulet P, Ehret-Sabatier L. Proteomic analysis of the systemic immune response of Drosophila. *Mol. Cell Proteomics* 2004; **3**: 156–166.

56. Yoshiga T, Georgieva T, Dunkov BC, Harizanova N, Ralchev K, Law JH. Drosophila melanogaster transferrin. Cloning, deduced protein sequence, expression during the life cycle, gene localization and up-regulation on bacterial infection. *Eur. J. Biochem.* 1999; **260**: 414–420.

57. Stafford JL, Neumann NF, Belosevic M. Products of proteolytic cleavage of transferrin induce nitric oxide response of goldfish macrophages. *Dev. Comp. Immunol.* 2001; **25**: 101–115.

58. Gomme PT, McCann KB, Bertolini J. Transferrin: structure, function and potential therapeutic actions. *Drug Discov. Today* 2005; **10**: 267–273.

59. Hanzawa H, Shimada I, Kuzuhara T, Komano H, Kohda D, Inagaki F, Natori S, Arata Y. H-1 nuclear-magnetic-resonance study of the solution conformation of an antibacterial protein, sapecin. *FEBS Lett.* 1990; **269**: 413–420.

60. Yamada K, Natori S. Purification, Sequence and antibacterial activity of 2 novel sapecin homologs from *Sarcophaga* embryonic-cells – similarity of sapecin-B to charybdotoxin. *Biochem. J.* 1993; **291**: 275–279.

61. Matsuyama K, Natori S. Purification of three antibacterial proteins from the culture medium of NIH-Sape-4, an embryonic cell line of *Sarcophaga peregrina*. *J. Biol. Chem.* 1988; **263**: 17112–17116.

62. Yamada K, Natori S. Purification, sequence and antibacterial activity of two novel sapecin homologues from *Sarcophaga* embryonic cells: similarity of sapecin B to charybdotoxin. *Biochem. J.* 1993; **291**(Pt 1): 275–279.